Torus-Bifurcation Mechanisms in a DC/DC Converter With Pulsewidth-Modulated Control

Zhanybai T. Zhusubaliyev, Erik Mosekilde, and Olga O. Yanochkina

***Abstract*—Pulse-modulated converter systems play an important role in modern power electronics. However, by virtue of the complex interplay between ordinary (smooth) and so-called border-collision bifurcations generated by the switching dynamics, the changes in behavior that can occur in multilevel converter systems under varying operational conditions still remain to be explored in full. Considering the dynamics of a three-level dc/dc-converter, we demonstrate a number of new scenarios for the birth or destruction of resonant and ergodic tori. One scenario involves the formation of a doubled-layered torus structure around a stable focus point through three subsequent border-collision fold bifurcations. Another scenario replaces one of the fold bifurcations by a global bifurcation. In both of these scenarios, the basic mode of the converter remains stable while other modes grow up and bifurcate around it. We also illustrate the subcritical birth of both an ergodic and a resonance torus from the basic operational mode.**

***Index Terms*—Border-collision bifurcations, piecewise-smooth dynamical systems, quasi-periodicity, torus-birth bifurcations.**

I. Introduction

During the last couple of decades, pulse-modulated converted systems have gradually superseded more conventional power supply systems for a broad range of applications in the transport sector as well as in the industry and the private households [1], [2]. DC/DC converters represent one of the most commonly used converter systems. To provide an adjustable voltage (or current) to a load with a fixed input voltage, power transistors and other active devices are made to operate in switching mode in a feedback circuit that also involves passive components such as power diodes, resistors, capacitors, and inductors. The use of a relatively high switching frequency allows the size and weight of many of the passive components to be reduced and this, in general, also reduces the price of the converter. The conversion efficiency that one can achieve with this kind of systems typically falls in the 80–90% range [1], [2].

The simplest form of a dc/dc converter operates with a single external voltage supply that is connected to or disconnected from the load via a couple of switches and an *LC*-filter. The switching process is regulated via a feedback control that compares the realized load voltage with a desired reference value. If the attained voltage is too small, the fraction of time that the load is connected to the external supply voltage is increased, and vice versa. Higher feedback gain will generally improve the accuracy by which the desired output voltage is achieved, but will also affect the stability of both the operational mode and other possible modes in the system. Our aim of this paper is to examine the type of transitions that can occur as the feedback gain is increased beyond normal operational conditions.

Multilevel converters make use of two or more input levels for the supply voltage. The desired output voltage can then be produced with higher efficiency and less distortion [2]–[8]. The presence of several input levels may also allow the voltage and frequency requirements to the components to be reduced. The main disadvantage of this type of system is obviously the added complexity that follows with the increased number of components [2].

Pulse-modulated control destroys the smoothness of the system. Each time a switching occurs, the system starts a new trajectory with a dynamics determined by the new circuit topology and with initial conditions that depend on continuation criteria determined by the switching process. The trajectory will then consist of a sequence of curves with each curve describing the smooth dynamics between two switching processes, but with nonsmooth transitions from curve to curve. In many cases, the system may be linear between two switching processes, and the description of the time-continuous system can then be reduced to a time-discrete mapping that relates the state immediately before one switching process to the state of entrance to the previous switching. A classic example of this type of dynamics is the deterministic description of die tossing in terms of alternating flight and collision maps [9], [10].

The mapping that results from the earlier procedure is not linear, but typically involves boundaries between regions in phase space where the underlying dynamics is different. Under variation of a parameter, a fixed point of the mapping (or a point of a periodic orbit) may cross the boundary between two such regions. This, in general, leads to an abrupt change in the eigenvalues of the fixed point (or periodic orbit) and, hence, to a sudden change in its stability. The switching process in this way gives rise to a new class of bifurcation phenomena, the so-called border-collision bifurcations [11]–[21] that are clearly

Manuscript received June 12, 2010; revised August 22, 2010; accepted December 4, 2010. Date of current version June 10, 2011. This work was partially supported by the Federal Target Programme " Scientific and Pedagogical Personnel of Innovative Russia" for 2009–2013 (" Mechanics," Contract No. П2228). Recommended for publication by Associate Editor E. Santi.

Z. T. Zhusubaliyev is with the Department of Computer Science, Kursk State Technical University (South West State University), Kursk 305040, Russia (e-mail: zhanybai@hotmail.com).

E. Mosekilde is with the Department of Physics, Technical University of Denmark, Lyngby 2800, Denmark (e-mail: erik.mosekilde@fysik.dtu.dk).

O. O. Yanochkina is with the Department of Computer Science, Kursk State Technical University (South West State University), Kursk 305040, Russia (e-mail: yanoolga@gmail.com).

Color versions of one or more of the figures in this paper are available online at http://ieeexplore.ieee.org.

Digital Object Identifier 10.1109/TPEL.2010.2100830

distinguishable from the transitions we know from smooth systems. It is well known, for instance, that border-collision bifurcations can give rise to direct transitions from a stable fixed point to deterministic chaos or from a fixed point to a cycle of any periodicity [17], [19]. It has also been demonstrated that a border-collision fold bifurcation (the analog of a saddle-node bifurcation in smooth systems) can give rise to the simultaneous appearance of a pair of saddle and stable (or unstable) focus cycles [19], [22].

Lack of smoothness may also cause the classic smooth bifurcations to change character such that, for instance, the period-2 solution in a period-doubling bifurcation arises abruptly and with finite amplitude. We have previously investigated a variety of different nonlinear dynamic phenomena that can occur in dc/dc converters with pulsewidth modulation (PWM) [17], [22]–[28]. Part of this study has focused on the mechanisms by which border-collision bifurcations can lead to the appearance of quasi-periodic or synchronized periodic dynamics as a pair of complex conjugated Floquet multipliers (eigenvalues for the time-discrete mapping) of a stable periodic orbit jumps from the inside to the outside of the unit circle in the complex plane. Such processes represent the nonsmooth analog of a classical Neimark–Sacker bifurcation (Hopf bifurcation for maps). However, by contrast to the parabolic growth of the torus diameter with the distance to the bifurcation point observed for the Neimark–Sacker bifurcation, the border-collision torus-birth bifurcation leads to a linear growth in diameter. In collaboration with Banerjee and his cooperators [26], [29], we have recently shown experimentally that torus formation can take place in a realistic converter system, and we have also investigated a number of different processes by which torus destruction can occur in nonsmooth systems [25], [26], [30].

More recently, we have studied the formation and destruction of multilayered resonance tori, i.e., of tori with several interconnected layers of manifolds that link different stable and unstable cycles [25]. We have shown that such structures can also arise in smooth dynamical systems through period-doubling (or pitchfork) bifurcations in a direction transverse to the manifold of the original resonance torus [31]–[34]. An essential condition for this type of structure to be observed is that the considered system has a dimension that is high enough for transitions transverse to the torus manifold to take place.

Our previous investigations of nonlinear dynamic phenomena in dc/dc converter systems have focused on the regime of intermediate feedback gain factors. This is the regime where one can observe ergodic and resonant torus dynamics produced through Neimark–Sacker and by supercritical border-collision torus-birth bifurcations. Both of these processes lead to destabilization of the basic operational mode as a pair of complex conjugated multipliers move out of the unit circle. This implies that the bifurcation points can be predicted by a linear stability analysis of this mode.

The purpose of this paper is to initiate a study of the bifurcation processes that take place at higher values of the corrector gain factor where the model displays a much more complicated distribution of modes and where new types of torus-birth bifurcations take place. Our first scenario involves the formation of a double-layered torus structure around the stable focus point through a series of three subsequent border-collision fold bifurcations. This leads to the coexistence of a period-10 resonance mode with the basic operational mode, a result that is verified through direct simulation of the circuit model. In the second scenario, one of the fold bifurcations is replaced by a global bifurcation, but again the basic operational mode maintains its stability. We conclude the present investigations by demonstrating the formation of both resonant and ergodic tori through subcritical border-collision torus-birth bifurcations, a type of bifurcation that we only observe at high corrector gain factors.

Many other fields of engineering are also characterized by the widespread occurrence of systems of a nonsmooth nature. Besides in power supply systems, on–off regulation is also applied for the control of boilers, freezers, refrigerators, etc., and, as described earlier, the topology, and hence the dynamics of such systems, changes abruptly each time a switching occurs. In mechanical engineering, lack of smoothness is associated with all problems that involve impacts or stick–slip friction. This includes metal cutting and other forms of material processing [35], [36], the motion of railroad wheel sets [37] and rotating machines with final clearances [38], and many other systems as well.

Economic and managerial systems may be considered to exhibit very similar phenomena if they involve well-defined intervention thresholds. Decisions to hire new employees or acquire additional production capacity may change abruptly from a situation with growing demand to one of surplus production and rising inventories. The piecewise linear model of a cascaded production–distribution system has thus been found to display bifurcation phenomena very similar to those presented here [10], [39].

II. Power-Electronic Converter With Multilevel Control

In order to examine the dynamics of a pulse-modulated control system when the operational conditions approach the region of high feedback gain, let us consider the multilevel dc/dc converter sketched in Fig. 1(a). Here, N is the number of input levels for the voltage supply, and E_0 denotes the highest available input voltage. As aforementioned, the advantage of using several input levels is that the desired output voltage can be provided with high efficiency and relatively little distortion. Multilevel converter systems are, therefore, becoming quite common, particularly for applications that require significant versatility. In the following calculations, we shall take the number of levels to be $N = 3$.

Considering again the control diagram in Fig. 1(a), R is the load resistance, E_r the output voltage, and L the inductance of the filter coil. CS is the current sensor, β its sensitivity, and $V_{\rm ref}$ the reference voltage. R_0 and C_0 are components of the integrating corrector circuit, DA_0 is the corrector amplifier, and α the corrector gain factor. S/H is a sample-and-hold unit that reads the error signal αx_2 at every clock time and maintains it for the following switching period (see Fig. 1(b) for an explanation of the temporal aspects of the control). Finally, the

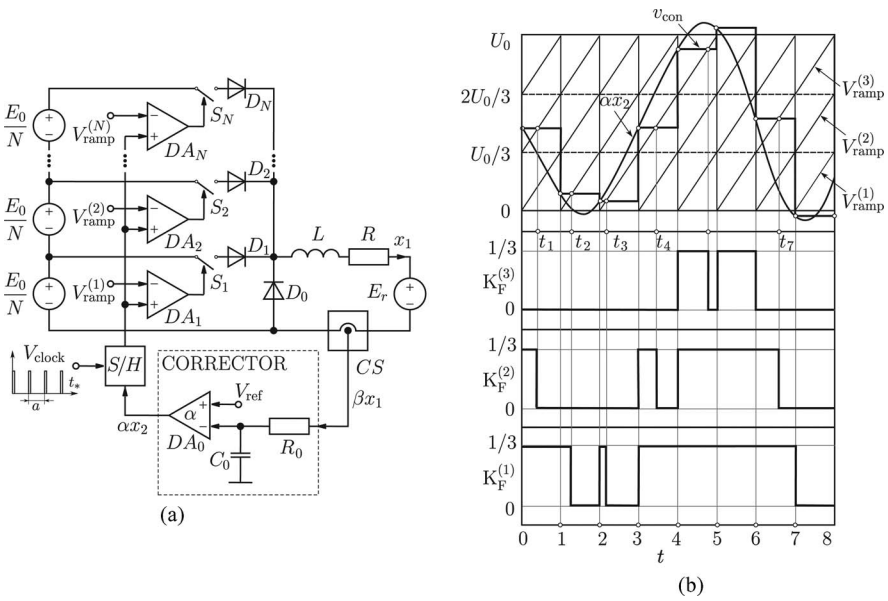

Fig. 1. (a) Schematic diagram of the considered dc/dc converter. E_0 is the maximum available input voltage, N the number of input levels, and R the load resistance. E_r is the output voltage and $V_{\rm ref}$ the reference voltage. CS is the current sensor, R_0, C_0, and DA_0 are components of the feedback control, and S/H is a sample-and-hold unit that generates the control signal to the comparators $DA_1, DA_2, \ldots, DA_N$. (b) Temporal variation of the control signal to illustrate the generation of the switching signals. $v_{\rm con}$ is the output signal from the sample-and-hold unit and $V^{(s)}_{\rm ramp}$, $s = 1, 2, \ldots, N$, are the ramp signals for the three different zones.

comparators DA_s, $s = 1, 2, \ldots, N$, compare the output signal from the sample-and-hold unit with the sawtooth signals $V^{(s)}_{\rm ramp}$, $s = 1, 2, \ldots, N$, in order to generate the control signals to the switches $S_1, S_2, \ldots, S_N$.

For a three-level system, the feedback control is implemented by means of three ramp functions such that $V^{(1)}_{\rm ramp}$ varies from 0 to $U_0/3$, $V^{(2)}_{\rm ramp}$ between $U_0/3$ and $2U_0/3$, and $V^{(3)}_{\rm ramp}$ between $2U_0/3$ and U_0. All three ramp functions are driven by the same clock. Fig. 1(b) illustrates the generation of the switching signals. At the beginning of each ramp cycle, the sample-and-hold unit reads the corrector output signal αx_2 and maintains this value for the entire ramp cycle. The output voltage from the sample-and-hold unit is denoted $v_{\rm con}$. As long as the value of $v_{\rm con}$ (the control signal) falls in the interval from 0 to $U_0/3$ (the first zone), it is compared with $V^{(1)}_{\rm ramp}$. If $v_{\rm con}$ exceeds $V^{(1)}_{\rm ramp}$, the switch S_1 is connected to the input voltage $E_0/3$, and the connection is broken as soon as $V^{(1)}_{\rm ramp}$ becomes larger than $v_{\rm con}$. A similar scheme is applied if $v_{\rm con}$ falls in one of the other zones.

The dynamics of the three-level converter system may be represented by the following set of two-coupled nonautonomous differential equations with discontinuous right-hand sides:

$$\dot{x} = \lambda_1 x + \gamma(\Omega_m K_{\rm F} - \Omega_r), \quad \dot{y} = -x + \lambda_2 y + 1. \qquad (1)$$

Here

$$K_{\rm F} = \sum_{s=1}^{N} K_{\rm F}^{(\rm s)}$$

with

$$K_{\rm F}^{(\rm s)} = \frac{1}{2N}\left(1 + {\rm sign}\xi_{\rm s}\right), \qquad \xi_{\rm s} = y(\tau) + \eta_{\rm s}(t)$$

$$\eta_{\rm s}(t) = \frac{V_{\rm ramp}(t_*)}{\alpha\lambda_2 V_{\rm ref}} = \frac{q}{N\alpha\lambda_2}\left(s - 1 + t - \tau\right)$$

and

$$x = \frac{\beta x_1}{V_{\rm ref}}, \qquad y = -\frac{x_2}{\lambda_2 V_{\rm ref}}, \qquad \lambda_1 = -\frac{aR}{L}$$

$$\lambda_2 = -\frac{a}{C_0 R_0} \qquad \gamma = \frac{a\beta}{L}, \qquad \Omega_m = \frac{E_0}{V_{\rm ref}}$$

$$\Omega_r = \frac{E_r}{V_{\rm ref}}, \qquad t = t_*/a, \qquad q = \frac{U_0}{V_{\rm ref}}.$$

The (dimensionless) dynamic variables x and y represent the normalized load current x_1 and the error signal x_2 of the integrating feedback corrector, respectively. The sawtooth functions $\eta_{\rm s}(t)$, $s = 1, 2, \ldots, N$, are periodically repeated normalized ramp functions with the ramp period 1, i.e., $\eta_{\rm s}(t+1) \equiv \eta_{\rm s}(t)$. Here, t is a dimensionless time variable while N, as before, is the number of zones. The parameter q controls the amplitude of the sawtooth functions. $\tau = [t] = k - 1$, $k = 1, 2, \ldots$, is the discrete time variable, $[t]$ being defined as a function that is equal to the integer value of its argument. The function $y(\tau)$, therefore, represents the error signal of the integrating feedback corrector at the beginning of each ramp cycle.

Ω_m and Ω_r are the input and output voltages, normalized relative to the reference signal $V_{\rm ref}$. α is the corrector amplification constant. In the following bifurcation analysis, we shall consider α and Ω_r as control parameters. Based on the electronic parameters of a typical converter [19], we have chosen $E_0 = 100$ V, $R = 0.083\,\Omega$, $L = 0.0106$ H, $U_0 = 10$ V, $V_{\rm ref} = 5$ V, $\beta = 0.1\,\Omega$, $a = 2 \times 10^{-3}$ s, $C_0 R_0 = 10^{-2}$ s, $N = 3$, $\alpha > 0$, and $E_r > 0$.

In order to proceed with the problem, let us illustrate how one can construct a stroboscopic mapping for the periodically driven time-continuous system (1). The use of such maps, rather than trying integrate the equations of the motion (1) numerically, reduces the required computer time by orders of magnitude. However, to be complete, we shall illustrate the full congruence of the two approaches through a direct simulation of the time continuous system for one of the transitions presented in the next section.

It follows from the expression for the control pulse [see Fig. 1(b)] that during the ramp period $k-1<t<k$, $k=1,2,\ldots$,

$$K_{\rm F}=\begin{cases}\dfrac{s_k}{N}, & k-1<t<t_k\\ \dfrac{s_k-1}{N}, & t_k<t<k\end{cases}$$

where the switching time t_k is determined as the time at which the error signal $v_{\rm con}$ crosses through one of the ramp function $V_{\rm ramp}^{(s)}$, $s=1,2,3$. The integer s_k denotes the zone in which the intersection takes place.

During the interval $k-1<t<t_k$, system (1) attains the form

$$\dot{x}=\lambda_1 x+\gamma\left(\frac{s_k}{N}\Omega_m-\Omega_r\right),\quad \dot{y}=-x+\lambda_2 y+1$$

with the solution

$$x(t)=e^{\lambda_1(t-k+1)}(x_{k-1}+\vartheta_k^+)-\vartheta_k^+$$

$$y(t)=\frac{e^{\lambda_1(t-k+1)}-e^{\lambda_2(t-k+1)}}{\lambda_2-\lambda_1}\times(x_{k-1}+\vartheta_k^+)+e^{\lambda_2(t-k+1)}(y_{k-1}+\theta_k^+)-\theta_k^+$$

or evaluated at the switching time $t=t_k$

$$x(t_k)=e^{\lambda_1(t_k-k+1)}(x_{k-1}+\vartheta_k^+)-\vartheta_k^+$$

$$y(t_k)=\frac{e^{\lambda_1(t_k-k+1)}-e^{\lambda_2(t_k-k+1)}}{\lambda_2-\lambda_1}\times(x_{k-1}+\vartheta_k^+)+e^{\lambda_2(t-k+1)}(y_{k-1}+\theta_k^+)-\theta_k^+.$$

Here, x_{k-1} and y_{k-1} denote the values of the dynamic variables x and y at the switching time $k-1$. The integration constants ϑ_k^+ and θ_k^+ are given by

$$\vartheta_k^+=\frac{\gamma}{\lambda_1}\left(\frac{s_k}{N}\Omega_m-\Omega_r\right)\quad\text{and}\quad\theta_k^+=\frac{\vartheta_k^++1}{\lambda_2}.$$

In the subsequent time interval $t_k<t<k$, system (1) takes the form

$$\dot{x}=\lambda_1 x+\gamma\left(\frac{s_k-1}{N}\Omega_m-\Omega_r\right),\quad \dot{y}=-x+\lambda_2 y+1$$

with the solution

$$x(t)=e^{\lambda_1(t-t_k)}\left(x(t_k)+\vartheta_k^-\right)-\vartheta_k^-$$

$$y(t)=\frac{e^{\lambda_2(t-t_k)}-e^{\lambda_1(t-t_k)}}{\lambda_1-\lambda_2}\times\left(x(t_k)+\vartheta_k^-\right)+e^{\lambda_2(t-t_k)}\left(y(t_k)+\theta_k^-\right)-\theta_k^-.$$

Hence, for $t=k$

$$x_k=e^{\lambda_1(k-t_k)}\left(x(t_k)+\vartheta_k^-\right)-\vartheta_k^-$$

$$y_k=\frac{e^{\lambda_2(k-t_k)}-e^{\lambda_1(k-t_k)}}{\lambda_1-\lambda_2}\times\left(x(t_k)+\vartheta_k^-\right)+e^{\lambda_2(t-t_k)}\left(y(t_k)+\theta_k^-\right)-\theta_k^-.$$

Here, x_k and y_k denote the values of the dynamic variables x and y at the switching time k. The integration constants ϑ_k^- and θ_k^- are determined by

$$\vartheta_k^-=\frac{\gamma}{\lambda_1}\left(\frac{s_k-1}{N}\Omega_m-\Omega_r\right)\quad\text{and}\quad\theta_k^-=\frac{\vartheta_k^-+1}{\lambda_2}.$$

After inserting the expressions for $x(t_k)$ and $y(t_k)$, the equations for the map are obtained in form

$$\begin{aligned}x_k&=e^{\lambda_1}(x_{k-1}+\vartheta_k^+)+\lambda_2\mu e^{\lambda_1(1-z_k)}-\vartheta_k^-\\ y_k&=\frac{e^{\lambda_1}-e^{\lambda_2}}{\lambda_2-\lambda_1}((x_{k-1}+\vartheta_k^+)+e^{\lambda_2}(y_{k-1})+\theta_k^+)\\&\quad+\mu\frac{\lambda_2 e^{\lambda_1(1-z_k)}-\lambda_1 e^{\lambda_2(1-z_k)}}{\lambda_2-\lambda_1}-\theta_k^-\end{aligned}\tag{2}$$

with $\mu=\dfrac{\gamma\Omega_m}{N\lambda_1\lambda_2}$.

As aforementioned, the integer s_k represents the zone in which the switching in the kth ramp cycle takes places. The variable z_k represents the relative pulse duration in the kth ramp cycle: $z_k=t_k-k+1$, $0\le z_k\le 1$. These two intermediate variables are determined by

$$z_k=\begin{cases}0, & y_{k-1}<0\\ 1, & y_{k-1}>-\dfrac{q}{\alpha\lambda_2}\\ -\dfrac{N\alpha\lambda_2}{q}y_{k-1}-s_k+1, & 0\le y_{k-1}\le-\dfrac{q}{\alpha\lambda_2}\end{cases}$$

$$s_k=\begin{cases}1, & y_{k-1}<0\\ N, & y_{k-1}>-\dfrac{q}{\alpha\lambda_2}\\ \left[-\dfrac{N\alpha\lambda_2}{q}y_{k-1}\right]+1, & 0\le y_{k-1}\le-\dfrac{q}{\alpha\lambda_2}\end{cases}$$

where

$$\left[-\frac{N\alpha\lambda_2}{q}y_{k-1}\right]$$

again is defined as a function that is equal to the integer value of its argument.

III. Distribution of Modes

Fig. 2 provides an overview of the distribution of dynamical modes (i.e., steady-state solutions to the equations of motion) in the (α,Ω_r)-plane. We recall that α is the corrector gain factor and Ω_r the normalized output voltage. The figure considers a part of parameter space where the corrector gain factor is relatively high ($\alpha>5.0$). This implies that the converter is operating in a regime where instabilities are likely to arise. As aforementioned, the purpose of this investigation is to examine

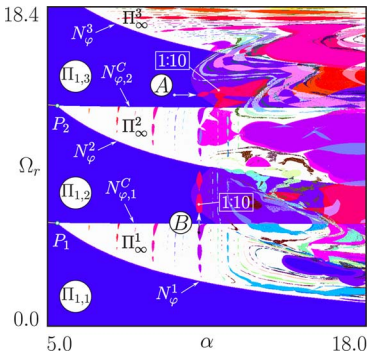

Fig. 2. Chart of dynamical modes in the (α, Ω_r) parameter plane. α is the corrector gain factor and Ω_r is the normalized output voltage. The blue regions represent stable periodic switching dynamics associated with operation at each of the three levels for the input voltage. The white regions represent 2-D torus dynamics with their characteristic sausage-on-a-string resonance zones. For gain factors exceeding 11, this relatively simple structure is overshadowed by an exceedingly complex structure of coexisting modes. This is the region of interest to this study.

the transitions that take place for $\alpha > 11$ where the relatively simple structure of blue and white regions is replaced by a much more complicated structure with several coexisting modes.

The blue domains denoted $\Pi_{1,1}$, $\Pi_{1,2,}$, and $\Pi_{1,3}$ represent operational regimes where the converter displays stable period-1 solutions. These are the normal operational modes. In the part of parameter space, we consider they are of focus type. This implies that they have damped oscillatory transients controlled by complex conjugate eigenvalues with numerical values less than 1. The three domains correspond to the three levels of input voltage.

In the domain $\Pi_{1,1}$, the normalized output voltage Ω_r is relatively small and the converter can provide the required voltage through operation in the first zone, $v_{\rm con} < U_0/3$. In the domain $\Pi_{1,2}$, the system operates in the second zone, and for higher load voltages (in the domain $\Pi_{1,3}$) the converter operates in the third zone. The transition from one zone to another involves a border-collision bifurcation, either at the curve $N_{\varphi,1}^C$ or at the curve $N_{\varphi,2}^C$. At low values of the corrector gain factor (to the left of the points P_1 and P_2), this bifurcation takes form of a transition from one stable focus cycle to another. To the right of these points, the bifurcation involves the transition from a stable focus cycle (in the blue region) to an ergodic or resonant torus (in the white regions).

The curves N_φ^1, N_φ^2, and N_φ^3 are Neimark–Sacker bifurcation curves in which the stable period-1 solutions lose their stability and transform into closed invariant curves as the pair of complex conjugate eigenvalues continuously cross out through the unit circle in the complex plane. Above these curves, the converter displays ergodic dynamics (i.e., quasi-periodicity) intervened by an infinite number of domains where resonant dynamics occurs. This transition to torus dynamics takes place because the increasing feedback gain generates a second oscillatory mode in the system that interacts with the switching mode [29]. In Fig. 2, the quasi-periodic (or nonresonant) dynamics is found in the white areas of Π_∞^1, Π_∞^2, Π_∞^3, and the resonant two-mode dynamics is observed in the colored structures that run across these domains. The sausage-on-a-string shape of these structures is a characteristic feature of nonsmooth systems where the resonance zones are delineated by border-collision fold bifurcations [22]–[27].

The torus-birth bifurcations that take place as the converter crosses from stable periodic dynamics into one of the regions of (resonant or nonresonant) torus dynamics were discussed in several of our previous publications [24], [26]–[29]. These discussions were restricted, though, to the case of supercritical border-collision bifurcations. In this paper, we shall consider an example of a subcritical border-collision torus-birth bifurcation, a type of bifurcation that only occurs for $\alpha > 11$. Both the Neimark–Sacker and the border-collision torus-birth bifurcations proceed through destabilization of the stable focus cycle that exists in the dark blue regions, but the ways in which the torus amplitude grows as the working point moves deeper into the region of two-mode dynamics are quite different. Where the Neimark–Sacker bifurcation leads to a parabolic growth in torus amplitude, the growth is nearly linear for border-collision bifurcations [24], [26]–[28].

For $\alpha > 11$, the chart of dynamical modes displays much more complicated structure with several coexisting behaviors. The corrector gain is now so high that new modes begin to appear around the stable focus point (or the 2-D torus), and a variety of new bifurcation phenomena start to take place. The study of some of these phenomena is the subject of the following sections.

IV. New Mechanisms of Resonance-Torus Formation

The first new structure to appear as the corrector gain factor is increased beyond a value of about $\alpha = 11$ which is the vertically running red chain of period-10 domains. This chain appears like the continuation of the $1:10$ resonance domains that exist in the white regions with torus dynamics into the blue regions where the dynamics otherwise is indicated to be that of a regular periodic motion [stable fixed point of the map (2)]. However, this dynamics actually occur on a different torus.

Fig. 3 shows an example of how this new structure arises and develops as the corrector gain increases. Here, the gain factor changes from $\alpha = 11.225$ to $\alpha = 11.3$ along the direction A in Fig. 2. At the left edge of the resonance domain, a pair of period-10 node (N_0) and saddle (S_0) cycles are born in a border-collision fold bifurcation (the nonsmooth analog of a saddle-node bifurcation) while the original focus cycle F_* retains its stability [see Fig. 3(a)]. We note that the appearance of these new cycles cannot be predicted from a stability analysis of the main operational mode. They appear so to speak without warning. The converter now displays two stable periodic modes: the original period-1 focus cycle F_* that follows the switching process, and the newly born period-10 resonance node cycle N_0 that only repeats itself after ten switching cycles. The initial conditions will determine which mode the converter chooses with the stable manifold of the saddle cycle S_0 delineating the border of the two basins of attraction.

Inspection of Fig. 3(a) shows how the period-10 saddle and node cycles are arranged around the original period-1 focus

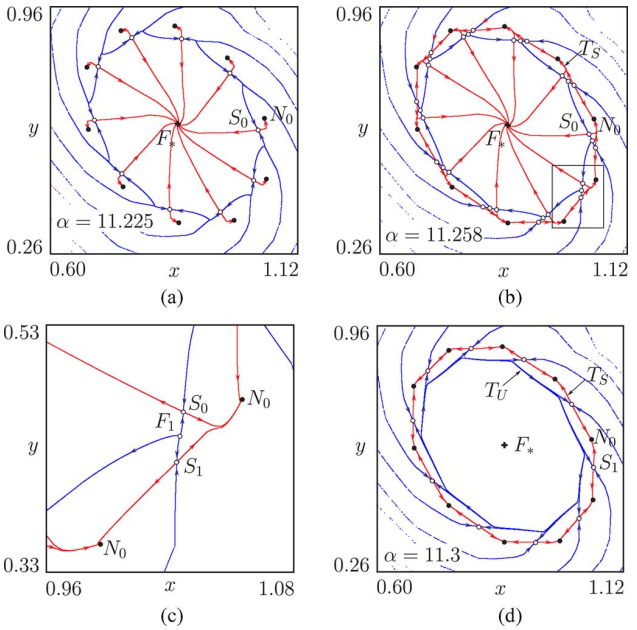

Fig. 3. Formation of two closed invariant curves through three subsequent border-collision fold bifurcations as the corrector gain factor is increased along the direction A in Fig. 2. (a) First bifurcation gives birth to the period-10 saddle and stable node cycles S_0 and N_0. (b) In the second bifurcation, the unstable focus cycle F_1 and the saddle cycle S_1 are born. (c) Unstable manifold of S_1 connects to N_0 and forms a stable resonance torus T_S. (d) Third border-collision fold bifurcation, involving the merger and annihilation of F_1 and S_0, leaves the unstable ergodic torus T_U as the basin boundary between the two coexisting stable cycles. $\Omega_r = 13.344$.

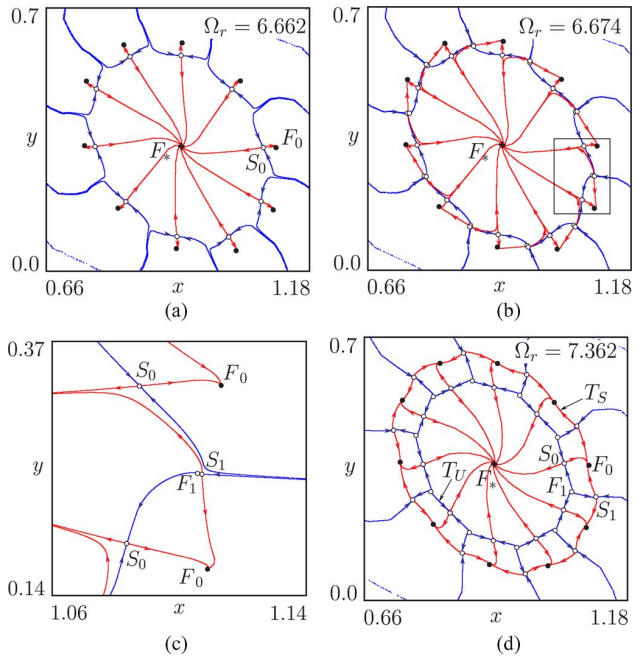

Fig. 4. Alternative route to the formation of two closed invariant curves. (a) After the first border-collision fold bifurcation, a pair of stable focus and saddle period-10 cycles F_0 and S_0 have appeared. (b) Second bifurcation produces a pair of saddle and unstable focus cycles S_1 and F_1. (c) Magnification of part of (b). (d) Phase portrait after reorganization of the structure through a heteroclinic bifurcation. The system now displays two nested resonance tori. $\alpha = 11.18$.

cycle, and how one branch of the unstable manifold to the saddle is connected directly to F_*. We thus conclude that the two period-10 cycles cannot be arranged along the invariant manifold of a torus structure.

As the corrector gain increases, a new pair of period-10 cycles (F_1 and S_1) is born in a second border-collision fold bifurcation and at a position in phase space relatively close to the existing period-10 cycles N_0 and S_0 [see Fig. 3(b)]. As illustrated in the blowup shown in Fig. 3(c), F_1 is an unstable focus. Moreover, the unstable manifold of S_1 connects to the stable node N_0. In this way, an attracting period-10 resonance torus T_S has been created through two subsequent border-collision fold bifurcations. The stable manifold to the saddle cycle S_0 continues to serve as the basin boundary between the two coexisting stable modes. Finally, Fig. 3(d) shows the phase portrait of the map (2) after a third (reverse) border-collision fold bifurcation in which the unstable period-10 focus cycle F_1 and the saddle period-10 cycle S_0 have merged and disappeared. This has lead to the birth of the repelling invariant closed curve (unstable torus) T_U, and this torus now separates the basins of attraction for the stable fixed point F_* and the stable period-10 resonance cycle N_0.

Fig. 4 illustrates an interesting variation to this scenario observed when the converter system enters the period-10 zone along the direction B in Fig. 2. Similar to the earlier scenario, the first border-collision fold bifurcation generates a stable period-10 cycle F_0 together with a period-10 saddle cycle S_0 [see Fig. 4(a)], but the stable period-10 cycle is now of focus type. The next border-collision fold bifurcation gives birth to the period-10 saddle and unstable focus cycles, S_1 and F_1, respectively [see Fig. 4(b)]. However, with one of the unstable manifolds of both saddle cycles S_0 and S_1 connecting to the stable period-1 focus F_*, the four coexisting period-10 cycles cannot yet be organized in a torus structure [see Fig. 4(c)]. Finally, Fig. 4(d) shows the reorganization of the phase portrait after a heteroclinic bifurcation in which the branch of the unstable manifold of S_1 that previously connected to F_* is directed toward F_0. This (third) bifurcation gives rise to the formation of a double-layered torus with an attracting resonance torus surrounding a repelling resonance torus of the same periodicity and with the unstable torus T_U representing the basin boundary between the two coexisting stable modes F_* and F_0.

The normal operational regime for the considered class of power electronic systems is the regime of period-1 mode operation. Different types of feedback correctors may be used in order to obtain a fast response, an accurate control, or a higher efficiency. However, in practice it is not easy to decide on the proper choice of the feedback corrector, the parameters of the converter, and the kind of PWM that can guarantee an operating mode with the desired dynamic characteristics. This becomes even more complicated by the fact that, under realistic conditions of operation, some parameters vary over time. Such variations may lead to the loss of stability of the period-1 operating mode and to the appearance of complex dynamical behaviors, including subharmonic, quasi-periodic, or chaotic oscillations (see Fig. 2).

Moreover, we have shown earlier (see Figs. 2–4) that multilevel converters can display situations where the normal

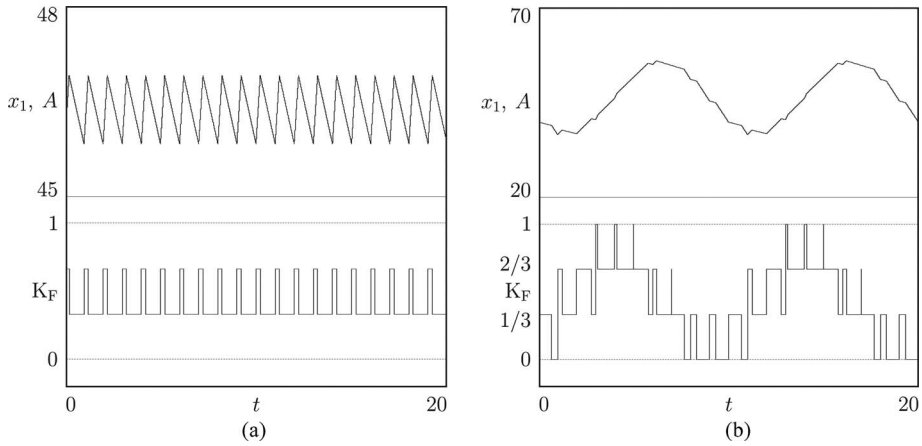

Fig. 5. Direct simulation of the circuit equation (1). Waveforms for the load current x_1 and control pulse K_F (a) for the basic operational (period-1) mode and (b) for the coexisting period-10 resonance dynamics. $\alpha = 11.18$ and $\Omega_r = 7.362$. The initial conditions determine which of the two waveforms the converter chooses. Note the dramatic difference in oscillation amplitude.

period-1 regime can coexist with stable ergodic or resonant dynamics over a significant range of parameter values. Under such conditions, the action of external noise, even of low intensity, can induce a sudden transition from the normal operation regime to the regime of torus (or chaotic dynamics). Such transitions can lead not only to the abrupt increase of the oscillation amplitude and the reduction of the control accuracy and of the efficiency [29], but also to the sudden breakdown of the system.

Fig. 5(a) shows the waveforms of the load current x_1 and the control pulses K_F under normal periodic operation (period-1 cycle) of our converter for the region between the bifurcation curves $\Omega^C_{\varphi,2}$ and Ω^2_φ where the stable period-1 mode coexists with the stable period-10 resonant dynamics [$\alpha = 11.18$ and $\Omega_r = 7.362$, see Fig. 4(d)]. In Fig. 5(a), the control pulse is produced by a comparator of the second zone. Fig. 5(b) shows the typical waveforms of the load current x_1 and of the control pulses K_F for the period-10 resonant dynamics. When comparing Fig. 5(a) and (b), one immediately notes that period-10 resonant dynamics involves a considerable increase of the oscillation amplitude. As illustrated in Fig. 4(c), the repelling torus T_U separates the basins of attraction of the coexisting motions.

V. Subcritical Border-Collision Bifurcations Leading to Torus Birth

As discussed in the Section I, we have previously examined different mechanisms of torus birth in piecewise smooth systems [24]–[29]. In particular, we have shown how the border-collision bifurcation at $N^C_{\varphi,1}$ (see Fig. 2) can give rise to the birth of resonant as well as ergodic tori [24], [26]–[29]. The border-collision mediated torus-birth bifurcation is distinguished from the classic Neimark–Sacker bifurcation by the fact that a pair of eigenvalues jump across the unit circle in the complex plane, rather than crossing it in a continuous manner.

The processes of torus birth through border-collisions that we have described so far have all been supercritical in nature. This means that a stable periodic orbit at one side of the bifurcation point is transformed into a stable torus on the other side. However, when the corrector gain factor in our converter exceeds approximately $\alpha = 11$, the torus-birth bifurcation becomes subcritical so that the bifurcation involves destabilization of a stable periodic cycle by a repelling torus that exists on the same side of the bifurcation point. In accordance with the well-known characteristics of a subcritical Neimark–Sacker bifurcation, the repelling torus subsequently stabilizes in a torus fold bifurcation.

The occurrence of such processes in the considered dc/dc converter is illustrated in Fig. 6. Fig. 6(a) shows the variation of the absolute value of the complex-conjugate multipliers of the fixed point F_*. We recall that this is the main operational mode of the converter. As the output voltage Ω_r increases through the Neimark–Sacker bifurcation point Ω^1_φ (corresponding to the bifurcation curve N^1_φ in Fig. 2), the pair of complex conjugated multipliers crosses the unit circle, and the multipliers remain numerically larger than 1 until the output voltage reaches the border-collision point at $\Omega^C_{\varphi,1}$. The interval from Ω^1_φ to $\Omega^C_{\varphi,1}$ corresponds to the white region between the corresponding torus-birth bifurcation curves in Fig. 2.

Fig. 6(b) displays the results of a 1-D bifurcation scan for $\alpha = 11.9$ with increasing values of the output voltage. We recognize the process of torus formation through a Neimark–Sacker bifurcation at Ω^1_φ. However, as inspection of the figure shows, the stable torus continues to exist as the system crosses the border-collision bifurcation point at $\Omega^C_{\varphi,1}$. By contrast, when the bifurcation scan is performed in the opposite direction [see Fig. 6(c)], we can follow the stable fixed point F_* all the way to the border-collision bifurcation point $\Omega^C_{\varphi,1}$ where the system abruptly jumps into a quasi-periodic orbit of finite amplitude.

To complete our discussion of border-collision torus bifurcations, Fig. 7 illustrates different aspects of a border-collision torus-birth bifurcation that takes place in the dc/dc converter for a corrector gain of $\alpha = 13.25$ as the point of operation crosses the border-collision bifurcation curve $N^C_{\varphi,1}$. Fig. 7(a) shows the variation in the absolute value of the complex conjugated multipliers for the fixed point. The fixed point is unstable to the right of the bifurcation point. Fig. 7(b) shows, besides the fixed point, the stable period-19 resonance cycle that coexists with the

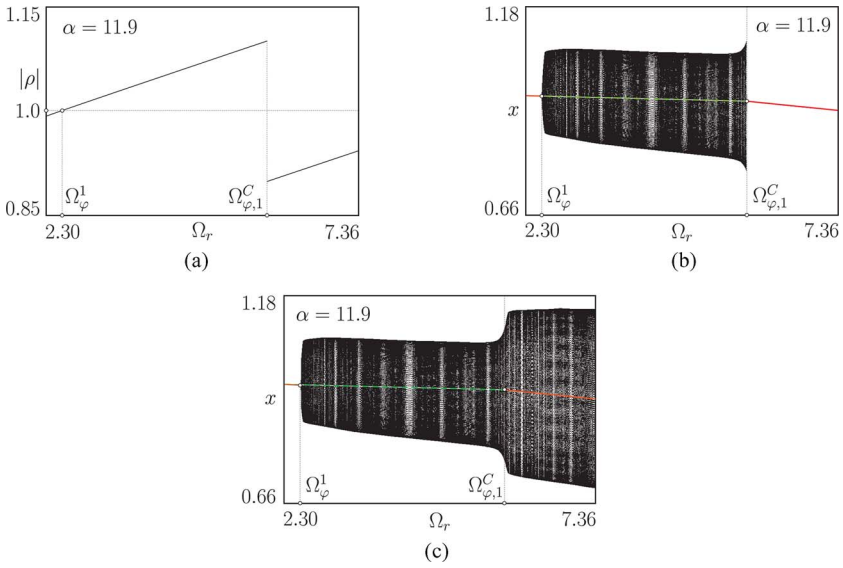

Fig. 6. Subcritical border-collision torus-birth bifurcation. (a) Variation of the absolute value $|\rho|$ of the complex conjugated multipliers $\rho_{1,2} = \rho_r \pm j\rho_j$ of the fixed point F_* through the Neimark–Sacker and the border-collision torus-birth bifurcations. (b), (c) 1-D bifurcation diagrams in the direction of increasing, respectively, decreasing, output voltages. Note the hysteresis and the abrupt jump in the diameter of the quasi-periodic attractor.

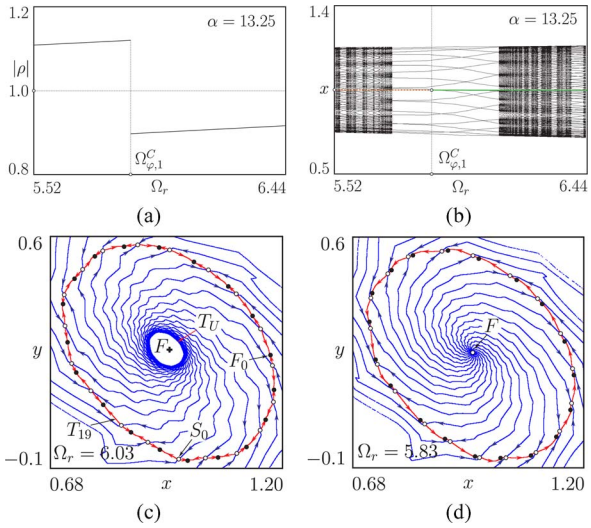

Fig. 7. Subcritical transition to a resonance torus through a border-collision bifurcation. (a) Variation of the absolute value $|\rho|$ of the complex conjugated multipliers of the fixed point F_*. (b) 1-D bifurcation diagram. Note the coexistence of the stable fixed point and the period-19 resonance cycle to the right in of the bifurcation point. (c) Phase portrait before the subcritical border-collision torus-birth bifurcation. (d) Phase portrait after the border-collision torus-birth bifurcation in which an unstable torus T_U merges with the focus fixed point F and disappears. $\alpha = 13.25$.

fixed point in an interval on both sides of the bifurcation point. Finally, Fig. 7(c) and (d) show phase portraits of the system as it approaches the bifurcation point from the right, and immediately after the bifurcation has occurred. This fixed point is now unstable, and the repelling torus has disappeared.

VI. Conclusion

The purpose of this paper was to examine some of the bifurcation phenomena that can arise in pulsewidth-modulated control systems as the feedback gain is turned up. Using the output voltage and the corrector gain factor as control parameters, we have performed a detailed analysis of the bifurcation structure for a realistic three-level dc/dc converter system. This has led us to observe a number of new torus-birth bifurcation mechanisms, including a couple of mechanisms that proceed through three subsequent border-collision fold bifurcations or through two border-collision fold bifurcations followed by a heteroclinic bifurcation. We have also studied the subcritical birth of a 2-D torus through a border-collision bifurcation.

At low values of the corrector gain factor ($\alpha < 5$), the system displays three different modes of operation, each corresponding to a stable period-1 cycle [or fixed point for the map (2)]. The regions of parameter space where these different modes exist are separated by border-collision bifurcations that represent the discrete transitions from one input voltage level to another.

As the corrector gain factor increases, new oscillatory modes tend to arise through instabilities generated by the feedback regulation. This gives rise to a set of Hopf bifurcations [or Neimark–Sacker bifurcations for the time discrete map (2)] in which transitions to resonant or ergodic two-mode dynamics occur. At the same time, the border-collision bifurcations delineating the three main zones of operation are transformed into torus-birth bifurcations. In the regions between these border-collision curves and the corresponding Hopf bifurcation curves, we observe quasi-periodic dynamics intervened by regions of resonance behavior. These latter regions display the characteristic sausage-on-a-string structure known to occur for piecewise smooth systems where the resonance zones are bounded by border-collision fold bifurcations.

When the corrector gain factor in our model exceeds a value of approximately 11, the torus-birth transitions that take place along the main border-collision bifurcation curves become subcritical. This implies that pairs of repelling and attracting tori continue to exist into the regions where a linear stability analysis

predicts that the main operational mode is stable, hence explaining the extension of the resonance regions into the areas where stable fixed point dynamics occurs and the appearance of new types of torus-birth bifurcations. We note that these transitions cannot be deduced from a linear stability analysis on the basic operational mode.

REFERENCES

[1] B. K. Bose, Ed., *Modern Power Electronics: Evolution, Technology, and Applications*. New York: IEEE Press, 1992, 2011.

[2] M. H. Rashid and F. L. Luo, Eds., *Power Electronics Handbook*. Amsterdam, The Netherlands: Elsevier, 2006.

[3] J. S. Lai and F. Z. Peng, "Multilevel converters: –A new breed of power converters," *IEEE Trans. Ind. Electron.*, vol. 32, no. 3, pp. 509–517, May/Jun. 1996.

[4] T. A. Meynard, H. Foch, P. Thomas, J. Courault, R. Jakob, and M. Nahrstaedt, "Multicell converters: Basic concepts and industry applications," *IEEE Trans. Ind. Electron.*, vol. 49, no. 5, pp. 955–964, Oct. 2002.

[5] R. Xinbo, L. Bin, C. Qianhong, T. Siew-Chong, and C. K. Tse, "Fundamental considerations of three-level DC-DC converters: Topologies, analyses, and control," *IEEE Trans. Circuits Syst. I, Reg. Papers*, vol. 55, no. 11, pp. 3733–3743, Dec. 2008.

[6] M. Shen, F. Z. Peng, and L .M. Tolbert, "Multilevel DC-DC power conversion system with multiple DC sources," *IEEE Trans. Power Electron.*, vol. 23, no. 1, pp. 420–426, Jan. 2008.

[7] J. Wen and K. M. Smedley, "Synthesis of multilevel converters based on single- and/or three-phase converter building blocks," *IEEE Trans. Power Electron.*, vol. 23, no. 3, pp. 1247–1256, May 2008.

[8] M. Hagiwara and H. Akagi, "Control and experiment of pulsewidth-modulated modular multilevel converters," *IEEE Trans. Power Electron.*, vol. 24, no. 7, pp. 1737–1746, Jul. 2009.

[9] R. Feldberg, M. Szymkat, C. Knudsen, and E. Mosekilde, "Iterated-map approach to die tossing," *Phys. Rev. A*, vol. 42, pp. 4493–4502, 1990.

[10] E. Mosekilde, *Topics in Nonlinear Dynamics: Applications to Physics, Biology and Economic*. Singapore: World Scientific, 1996.

[11] M. I. Feigin, "Doubling of the oscillation period with C-bifurcations in piecewise continuous systems," *PMM J. Appl. Math. Mech.*, vol. 34, pp. 861–869, 1970.

[12] H. E. Nusse and J. A. Yorke, "Border-collision bifurcations including "period two to period three" for piecewise smooth systems," *Physica D*, vol. 57, pp. 39–57, 1992.

[13] H. E. Nusse, E. Ott, and J. A. Yorke, "Border-collision bifurcations: An explanation for observed bifurcation phenomena," *Phys. Rev. E*, vol. 49, pp. 1073–1076, 1994.

[14] M. di Bernardo, M. I. Feigin, S. J. Hogan, and M. E. Homer, "Local analysis of C-bifurcations in n-dimensional piecewise-smooth dynamical systems," *Chaos, Solitons Fractals*, vol. 10, no. 11, pp. 1881–1908, 1999.

[15] G. H. Yuan, S. Banerjee, E. Ott, and J. A. Yorke, "Border-collision bifurcations in the buck converter," *IEEE Trans. Circ. Syst. I: Fund. Theory and Appl.*, vol. 45, no. 7, pp. 707–716, Jul. 1998.

[16] S. Banerjee, P. Ranjan, and C. Grebogi, "Bifurcations in two-dimensional piecewise smooth maps: Theory and applications in switching circuits," *IEEE Trans. Circuits Syst. I, Fundam. Theory Appl.*, vol. 47, no. 5, pp. 633–643, May 2000.

[17] Zh. T. Zhusubaliyev, E. A. Soukhoterin, and E. Mosekilde, "Border-collision bifurcations and chaotic oscillations in a piecewise-smooth dynamical system," *Int. J. Bifurcat. Chaos*, vol. 11, no. 12, pp. 2977–3001, 2001.

[18] S. Banerjee and G. C. Verghese, Eds., *Nonlinear Phenomena in Power Electronics*. New York: IEEE Press, 2001.

[19] Zh. T. Zhusubaliyev and E. Mosekilde, *Bifurcations and Chaos in Piecewise-Smooth Dynamical Systems*. Singapore: World Scientific, 2003.

[20] C. K. Tse, *Complex Behavior of Switching Power Converters*. Boca Raton, FL: CRC Press, 2003.

[21] M. di Bernardo, C. Budd, A. R. Champneys, P. Kowalczyk, A. B. Nordmark, G. Olivarand, and P. T. Piiroinen, "Bifurcations in nonsmooth dynamical systems," *SIAM Rev.*, vol. 50, pp. 629–701, 2008.

[22] Zh. T. Zhusubaliyev, E. A. Soukhoterin, and E. Mosekilde, "Border-collision bifurcations on a two-dimensional torus," *Chaos, Solitons Fractals*, vol. 13, no. 9, pp. 1889–1915, 2002.

[23] Zh. T. Zhusubaliyev, E. A. Soukhoterin, and E. Mosekilde, "Quasi-periodicity and border-collision bifurcations in a DC/DC converter with pulsewidth modulation," *IEEE Trans. Circuits. Syst. I, Fundam. Theory Appl.*, vol. 50, no. 8, pp. 1047–1057, Aug. 2003.

[24] Zh. T. Zhusubaliyev and E. Mosekilde, "Torus birth bifurcation in a DC/DC converter," *IEEE Trans. Circuits Syst. I, Regular Papers*, vol. 53, no. 8, pp. 1839–1850, Aug. 2006.

[25] Zh. T. Zhusubaliyev and E. Mosekilde, "Birth of bilayered torus and torus breakdown in a piecewise-smooth dynamical system," *Phys. Lett. A*, vol. 351, no. 3, pp. 167–174, 2006.

[26] Zh. T. Zhusubaliyev, E. Mosekilde, S. M. Maity, S. Mohanan, and S. Banerjee, "Border collision route to quasiperiodicity: Numerical investigation and experimental confirmation," *Chaos*, vol. 16, pp. 023122-1–023122-11, 2006.

[27] Zh. T. Zhusubaliyev and E. Mosekilde, "Direct transition from a stable equilibrium to quasiperiodicity in non-smooth systems," *Phys. Lett. A*, vol. 372, no. 13, pp. 2237–2246, 2008.

[28] Zh. T. Zhusubaliyev and E. Mosekilde, "Equilibrium-torus bifurcation in nonsmooth systems," *Physica D*, vol. 237, pp. 930–936, 2008.

[29] Zh. T. Zhusubaliyev, O. O. Yanochkina, E. Mosekilde, and S. Banerjee, "Two-mode dynamics in pulse-modulated control systems," *Annu. Rev. Control*, vol. 34, pp. 62–70, 2010.

[30] Zh. T. Zhusubaliyev, E. Mosekilde, S. De, and S. Banerjee, "Transition from phase-locked dynamics to chaos in a piecewise-linear map," *Phys. Rev. E*, vol. 77, no. 2, pp. 026206-1–026206-9, 2008.

[31] Zh. T. Zhusubaliyev and E. Mosekilde, "Formation and destruction of multilayered tori in cupled map systems," *Chaos*, vol. 18, no. 3, pp. 037124-1–037124-12, 2008.

[32] Zh. T. Zhusubaliyev and E. Mosekilde, "Multilayered tori in a system of two coupled logistic maps," *Phys. Lett. A*, vol. 373, pp. 946–951, 2009.

[33] Zh. T. Zhusubaliyev and E. Mosekilde, "Novel routes to chaos through torus breakdown in non-invertible maps," *Physica D*, vol. 238, pp. 589–602, 2009.

[34] Zh. T. Zhusubaliyev, J. L. Laugesen, and E. Mosekilde, "From multilayered resonance tori to period-doubled ergodic tori," *Phys. Lett. A*, vol. 374, pp. 2534–2538, 2010.

[35] R. I. Leine and H. Nijmeijer, *Dynamics and Bifurcations of Non-Smooth Mechanical Systems*. Berlin, Germany: Springer-Verlag, 2004.

[36] M. Wiercigroch, "Chaotic vibration of a simple model of the machine tool-cutting process system," *ASME J. Vibration Acoust.*, vol. 119, pp. 468–475, 1997.

[37] C. Knudsen, R. Feldberg, and H. True, "Bifurcations and chaos in a model of a rolling railway wheel set," *Philos. Trans. R. Soc. Lond. A*, vol. 338, pp. 455–469, 1992.

[38] S.-K. Choi and S. T. Noah, "Mode-locking and chaos in a Jeffcott rotor with bearing clearances," *J. Appl. Mech.*, vol. 61, pp. 131–138, 1994.

[39] E. Mosekilde and J. L. Laugesen, "Nonlinear dynamic phenomena in the beer model," *Syst. Dyn. Rev.*, vol. 23, pp. 229–252, 2007.

Zhanybai T. Zhusubaliyev received the Graduate degree from Tomsk State University for control systems and electronics (TUSUR), Tomsk, Russia, in 1982, the Ph.D. degree in electrotechnical systems from Tomsk State Politechnical University in 1989, and the Dr.Sc. degree in nonlinear dynamics in relay and pulsewidth-modulated control systems from Kursk State Technical University (South West State University), Kursk, Russia, in 2002.

From 1982 to 1992, he was a Scientist at the Research Institute of Automation and Electromechanics (RIAE), Tomsk. He is currently a Professor in the Department of Computer Science, Kursk State Technical University (South West State University). He is a coauthor of more than 80 scientific papers and several books, including the recent book *Bifurcations and Chaos in Piecewise-Smooth Dynamical Systems*(Singapore: World Scientific, 2003). His research interests include complex dynamics and chaos in piecewise-smooth systems, applications of nonlinear dynamics to power converters, and to relay and pulse control systems. He holds the inventor certificates for nine innovative constructions of relay control systems.

Erik Mosekilde received the M.Sc. degree in electrical engineering and the Ph.D. degree in solid-state physics both from the Technical University of Denmark (DTU), Lyngby, Denmark, in 1966 and 1968, respectively, and the Dr.Sc. degree in acoustoelectric instabilities from the University of Copenhagen, Copenhagen, Denmark, in 1977.

In 1970, he was a Postdoctoral Fellow at IBM Watson Research Center, Yorktown Heights, New York, and since then, he has been a Visiting Scientist at a number of different universities in Europe and North America. He is currently a Professor of biological applications of nonlinear dynamics. He is a coauthor of 210 scientific papers and of several books, including three recent books: *Topics in Nonlinear Dynamics* (Singapore: World Scientific, 1997), *Chaotic Synchronization* (Singapore: World Scientific, 2002), and *Bifurcations and Chaos in Piecewise-Smooth Dynamical Systems* (Singapore: World Scientific, 2003). His main research interests include modeling of complex systems and applications of nonlinear dynamics to physical, technical, and biological systems.

Olga O. Yanochkina received the Graduate degree from Kursk State Technical University (South West State University), Kursk, Russia, in 2001, where she is currently working toward the Ph.D. degree from the Department of Computer Science.

She is a coauthor of 12 scientific papers. Her research interests include complex dynamics in pulse-modulated control systems.